

## A Biohybrid Dynamic Random Access Memory

Jon Sinclair,<sup>†</sup> Daniel Granfeldt,<sup>†</sup> Johan Pihl,<sup>‡</sup> Maria Millingen,<sup>†</sup> Per Lincoln,<sup>†</sup>  
Cecilia Farre,<sup>‡</sup> Lena Peterson,<sup>§</sup> and Owe Orwar<sup>\*†</sup>*Contribution from the Department of Chemistry and Bioscience and Microtechnology Centre, Chalmers University of Technology, SE-412 96 Göteborg, Sweden, Collectricon AB, Fabriksgatan 7, SE-412 50 Göteborg, Sweden, and Department of Signal and Systems, Chalmers University of Technology, SE-412 96 Göteborg, Sweden*

Received November 29, 2005; E-mail: orwar@chembio.chalmers.se

**Abstract:** We report that GABA<sub>A</sub> receptors in a patch-clamped biological cell form a short-term memory circuit when integrated with a scanning-probe microfluidic device. Laminar patterns of receptor activators (agonists) provided by the microfluidic device define and periodically update the data input which is read and stored by the receptors as state distributions (based on intrinsic multistate kinetics). The memory is discharged over time and lasts for seconds to minutes depending on the input function. The function of the memory can be represented by an equivalent electronic circuit with striking similarity in function to a dynamic random access memory (DRAM) used in electronic computers. Multiplexed biohybrid memories may form the basis of large-scale integrated biocomputational/sensor devices with the curious ability to use chemical signals including odorants, neurotransmitters, chemical and biological warfare agents, and many more as input signals.

## Introduction

Short-term memory in the brain can be evoked and controlled by both pre- and postsynaptic factors.<sup>1–3</sup> GABA<sub>A</sub> receptors are chloride-selective inhibitory ion channels activated by GABA ( $\gamma$ -amino-*n*-butyric acid), the key inhibitory neurotransmitter in the central nervous system.<sup>4,5</sup> The receptor operates according to an intricate reaction scheme encompassing at least seven different states and 12 rate constants.<sup>6,7</sup> The GABA<sub>A</sub> receptor undergoes multiphasic and complex desensitization on rapid, slow, and intermediate time scales.<sup>7–10</sup> Recent studies have shown that repeated brief-period receptor activation leads to build-up of slowly desensitized states<sup>8</sup> in a concentration- and exposure time-dependent manner.<sup>11</sup>

In the present work, we developed an improved cyclic scanning patch-clamp (CSPC) method based on the combination of microfluidics and patch-clamp current recordings.<sup>12–14</sup> Specifically, in CSPC a patch-clamped cell is scanned back and forth

across fixed concentration gradients of receptor effectors provided by a microfluidic chip with control of each cycle with respect to exposure time ( $t_{\text{exp}}$ ), clearance time ( $t_{\text{wash}}$ ), and between cycle time ( $t_{\text{rest}}$ ). Using this technique we first show that the GABA<sub>A</sub> receptors themselves function as a short-term molecular memory. We then show that the memory can be accessed and refreshed by the input of specific patterns of agonist concentration and exposure time. In contrast to single channels, which will display a memory-less, stochastic behavior that can be described by Markov kinetics,<sup>15</sup> the memory presented here is an ensemble property that only can be observed in populations of ion channels. Finally, we show that ligand-activated GABA<sub>A</sub> ion channels under microfluidic control form a biohybrid memory circuit with function equivalent to a DRAM cell.

## Materials and Methods

**Microfluidic Set Up.** All electrophysiology experiments were performed using a commercially available microfluidic device for patch-clamp (Dynaflow 16, Collectricon AB, Göteborg, Sweden). The device used in this article has 16 channels of dimensions  $50 \times 60 \mu\text{m}$  ( $w \times h$ ) separated by  $22 \mu\text{m}$  thick walls at the point of exit into the open volume. The volume of the 16 sample reservoirs is  $80 \mu\text{L}$ , and the dimensions of the open volume are  $30 \times 35 \text{ mm}$ . Prior to experiments the device was loaded with different solutions using a micropipet. A 2 mm thick polycarbonate lid was attached over the sample reservoirs using double adhesive tape (3M, Stockholm, Sweden) in order to create a closed system. The lid was connected to a syringe with PE tubing, and a syringe pump (CMA/100, microinjection pump, Carnegie

<sup>†</sup> Department of Chemistry and Bioscience and Microtechnology Centre, Chalmers University of Technology.

<sup>‡</sup> Collectricon AB.

<sup>§</sup> Department of Signal and Systems, Chalmers University of Technology.

- (1) Destexhe, A.; Marder, E. *Nature* **2004**, *431*, 789–795.
- (2) Abbott, L. F.; Regehr, W. G. *Nature* **2004**, *431*, 796–803.
- (3) Zucker, R. S.; Regehr, W. G. *Annu. Rev. Physiol.* **2002**, *64*, 355–405.
- (4) Nusser, Z.; Hajos, N.; Somogyi, P.; Mody, I. *Nature* **1998**, *395*, 172–177.
- (5) Brickley, S. G.; Cull-Candy, S. G.; Farrant, M. *J. Neurosci.* **1999**, *19*, 2960–2973.
- (6) Jones, M. V.; Westbrook, G. L. *Neuron* **1995**, *15*, 181–191.
- (7) Haas, K. F.; Macdonald, R. L. *J. Physiol.* **1999**, *514*, 27–45.
- (8) Bianchi, M. T.; Macdonald, R. L. *J. Physiol.* **2002**, *544*, 3–18.
- (9) Jones, M. V.; Westbrook, G. L. *Trends Neurosci.* **1996**, *19*, 96–101.
- (10) Celentano, J. J.; Wong, R. K. *Biophys. J.* **1994**, *66*, 1039–1050.
- (11) Pugh, J. R.; Raman, I. M. *Biophys. J.* **2005**, *88*, 1740–1754.
- (12) Sinclair, J.; Pihl, J.; Olofsson, J.; Karlsson, M.; Jardemark, K.; Chiu, D. T.; Orwar, O. *Anal. Chem.* **2002**, *74*, 6133–6138.
- (13) Olofsson, J.; Pihl, J.; Sinclair, J.; Sahlin, E.; Karlsson, M.; Orwar, O. *Anal. Chem.* **2004**, *76*, 4968–4976.

- (14) Olofsson, J.; Bridle, H.; Sinclair, J.; Granfeldt, D.; Sahlin, E.; Orwar, O. *Proc. Natl. Acad. Sci. U.S.A.* **2005**, *102*, 8097–8102.
- (15) Hille, B. *Ion Channels of Excitable Membranes*, 3rd ed.; Sinauer Associates: Sunderland, MA, 2001.

Medicine, Cambridge, U.K.) was used to compress the air enclosed by the lid to initiate a well-defined pressure-driven flow in the channels, resulting in a flow velocity of 3 mm/s at the outlet.

**Cells.** Adherent WSS-1 cells stably expressing rat- $\alpha_1\beta_3\gamma_2$  GABA<sub>A</sub> receptors<sup>16</sup> were cultivated in Petri dishes for 4–8 days in (DMEM/F12) medium supplemented with antibiotics and antimycin (0.2%), fetal calf serum (10%), and L-glutamine. Before the experiments cells were washed and detached in a HEPES–saline buffer (HBS) containing (in mM) the following: 10 HEPES, 140 NaCl, 5 KCl, 1 CaCl<sub>2</sub>, 1 MgCl<sub>2</sub>, and 10 D-glucose (pH 7.4). All chemical used in the cell culturing were from Sigma-Aldrich (Sigma-Aldrich Sweden AB, Stockholm, Sweden).

**Electrophysiology.** Patch-clamp experiments were carried out in the whole-cell configuration (holding potential  $-40$  mV, sampling frequency 5 kHz, filter frequency 1 kHz). The cell bath solution (HBS) contained (in mM) 10 HEPES, 140 NaCl, 5 KCl, 1 CaCl<sub>2</sub>, 1 MgCl<sub>2</sub>, 10 D-glucose (pH 7.4). The patch-clamp electrode solution contained (in mM) 100 KCl, 2 MgCl<sub>2</sub>, 1 CaCl<sub>2</sub>, 11 EGTA, and 10 HEPES; pH was adjusted to 7.2 with KOH. All experiments were performed at room temperature (18–22 °C), and the microscope was placed in a Faraday cage to minimize electrical noise. For the CSPC experiments, we obtained dose–response curves where every second microchannel was loaded with 1, 5, 10, 20, 50, 100, and 500  $\mu$ M GABA, respectively, interdigitated with buffer solution for clearance after each agonist exposure. The experiments were performed using 10 different  $t_{\text{exp}}$  ranging from 30 ms to 10 s ( $n = 4$ –8 cells per  $t_{\text{exp}}$  scan), and the solution exchange time was 10–14 ms for the experimental conditions used. To ensure that all ligands had time to unbind from the receptor before a new scan was initiated, the recovery time in buffer,  $t_{\text{rest}}$ , was always  $>3$  min.

**Modeling of Receptor Kinetics.** The model was based on the CSPC protocol presented herein under the assumption of (pseudo) first-order microscopic rates. Let  $s$  be a vector with seven elements representing the relative concentrations of the different receptor states according to Figure 3A. Assuming a certain fixed GABA concentration, the rate laws describing the interconversion of the receptor states are all of (pseudo) first order and the matrix exponential of the corresponding matrix of rate constants can be used to solve the initial value problem

$$s(t) = \text{expm}(Kt) \cdot s_0 \quad (1)$$

where  $\text{expm}$  denotes the matrix exponential function, the vector  $s(t)$  contains the relative concentrations at time  $t$ , the vector  $s_0$  contains the starting concentrations,  $K$  is a  $7 \times 7$  matrix with the 12 rate constants of Figure 3A connecting the different states, and the three bimolecular rate constants are multiplied with the fixed GABA concentration. Simulated consecutive response curves were obtained by several applications of eq 1 with different GABA concentrations for each curve. The first starting concentration vector  $s_0$  was taken to be unity for the free receptor and zero elsewhere, and the last vector  $s(t)$  of the previous curve was taken as the new  $s_0$  starting vector for the next one. The calculations were performed with the Matlab software package (The MathWorks, Inc.).

For SPICE simulations, the equivalent circuit consisting of capacitors, resistors, and transconductors was inserted into a circuit analysis program using the SPICE simulation software tool HSPICE (Synopsys Inc., Mountain View, CA) and modeled for voltage protocols corresponding to the experimental protocols applied in the GABA dose–response experiments presented herein. Simulations were performed, and the output matched the output from the conventional kinetic model exactly.

## Results and Discussion

Experiments were performed in a 16-channel microfluidic device (Figure 1A) that enables the generation of a laminar

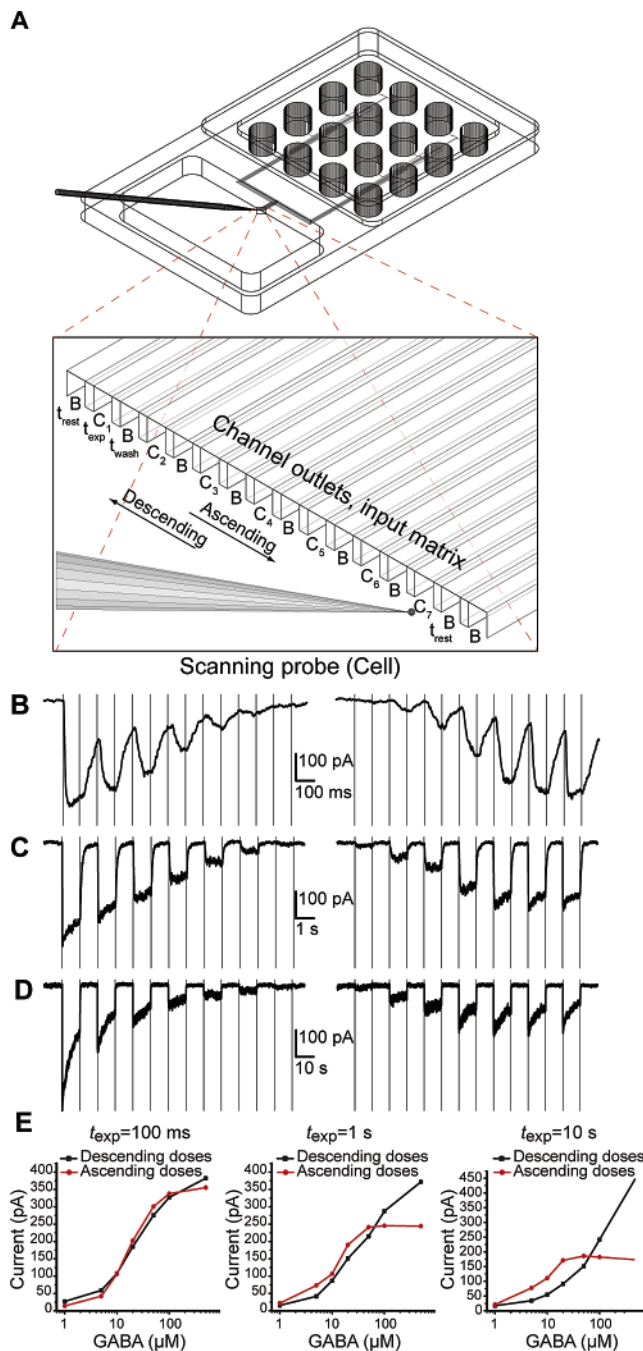


**Figure 1.** Schematic of the experimental setup and plots showing dose–response experiments obtained at different values of  $t_{\text{exp}}$ . (A) Overview of the device showing the 16 sample reservoirs connected to an open volume. The inset shows a magnified view of the channels exiting into the open volume, from where the different solutions are accessed by a patch-clamped cell. The loading pattern is chosen so that every second channel contains a specific ligand concentration ( $C_1, C_2, C_3, \dots, C_7$ ) to which the cell is exposed during a specified time ( $t_{\text{exp}}$ ) interdigitated with extracellular buffer (B) for washing the cell for a specified time ( $t_{\text{wash}}$ ). Before and after each scan the cell is held outside a channel for a recovery period defined as  $t_{\text{rest}}$ . (B–D) Patch-clamp current recordings obtained during descending (left) and ascending (right) doses of GABA (1, 5, 10, 20, 50, 100, and 500  $\mu$ M). Experiments shown are performed on the same cell with  $t_{\text{rest}} > 3$  min and  $t_{\text{exp}} = t_{\text{wash}}$ , which corresponds to the scale bar. (E) Exposure time and order of application modulates the dynamic range of GABA<sub>A</sub> receptor responses. Representative dose–response curves for  $t_{\text{exp}} = 100$  ms, 1 s, and 10 s. Initially, the responses are similar, displaying a sigmoidal appearance, but as  $t_{\text{exp}}$  increases the dose–response function changes shape.

(16) Davies, P. A.; Hoffmann, E. B.; Carlisle, H. J.; Tyndale, R. F.; Hales, T. G. *Neuropharmacology* **2000**, *39*, 611–620.

patterned flow of receptor agonists in the open volume.<sup>12,13,17</sup> We scanned the patch-clamped cells (expressing GABA<sub>A</sub> receptors) across the channel outlets in either ascending (low-to-high concentrations) or descending (high-to-low concentrations) order of dose application. Figure 1B–D displays examples of patch-clamp recordings obtained for doses applied in descending (left) and ascending order (right) where  $t_{\text{exp}}$  and  $t_{\text{wash}}$  were kept equivalent during each scan. From these recordings it is evident that the current response is a function of both application order and exposure time. Figure 1E shows peak-current dose–response curves obtained pairwise from the same cell for three different  $t_{\text{exp}}$ . When the receptors are titrated in ascending order we obtained, for all  $t_{\text{exp}}$  investigated, a classical sigmoidal dose–response function with a dynamic range of less than 2 orders of magnitude. For doses applied in descending order, a similar sigmoidal response function is obtained for  $t_{\text{exp}}$  less than 100 ms, whereas at longer times the response is nonsaturable and displays almost linear characteristics for the higher doses. However, when  $t_{\text{exp}}$  is less than 100 ms, which appears to be a characteristic phase transition time, the dose–response curves obtained in ascending order are close to identical to dose–response curves obtained in descending order (data not shown). These experiments demonstrate the existence of an activation-dependent molecular memory. The memory is caused by the receptors capability to enter inactive desensitized states, which will affect the total number of receptors available for opening. Thus, the input function,  $f(t_{\text{exp}}, [\text{GABA}], t_{\text{wash}})$ , will create state distributions in the receptors ( $n_{\text{O}}/n_{\text{tot}}$ ,  $n_{\text{C}}/n_{\text{tot}}$ ,  $n_{\text{D}}/n_{\text{tot}}$ , where  $n_{\text{O}}$ ,  $n_{\text{C}}$ , and  $n_{\text{D}}$  are the numbers of receptors in open, closed, and desensitized states) which in turn are functions of the microscopic rate constants as will be closely examined below.

To test the duration of the memory, two sets of experiments were performed with  $t_{\text{exp}} = 100$  ms or 3 s. The experiments were done as previously described with pulse trains applied in either ascending or descending concentration order followed by, after a specified time ( $t_{\text{rest}}$ ), a test pulse of 500  $\mu\text{M}$  GABA. The data were analyzed by comparing the difference between the test pulse and a normalizing control response (for a fully resensitized receptor) (Figure 2). For  $t_{\text{exp}} = 3$  s, in both ascending and descending applications, the duration of the memory was longer than 120 s ( $p < 0.05$ , Student's  $t$  test). For  $t_{\text{rest}} = 180$  s the memory is no longer present, and for  $t_{\text{exp}} = 100$  ms the duration of the memory is less than 15 s.

We used a reaction scheme for the GABA<sub>A</sub> receptor proposed by Jones et al.<sup>18</sup> modified by the rate constants from Lindquist et al.<sup>19</sup> (Figure 3A) and modeled the distribution of different channel conformations for a population of receptors with the matrix exponential method.<sup>20</sup> The simulations show that the distribution of different channel states varies depending on the order of dose application. In ascending order scans a low agonist concentration causes a majority of the receptor population to enter  $D_{\text{slow}}$  (Figure 3B). In descending order applications the initial application of high agonist concentration pushes the

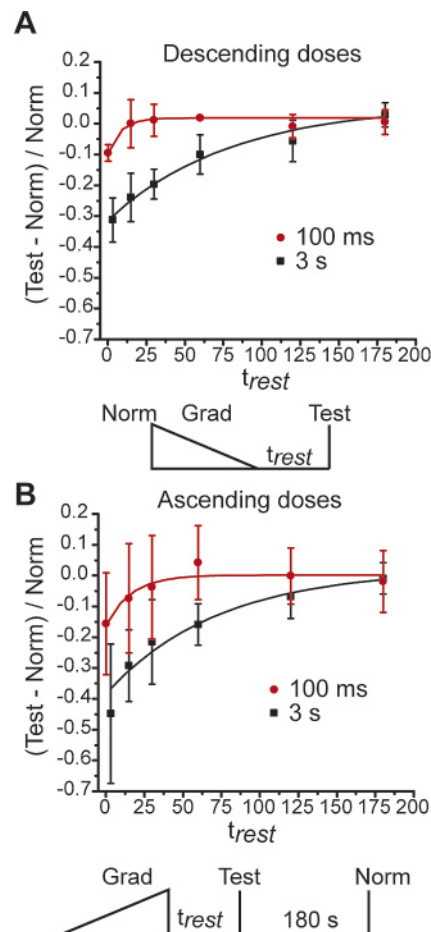


**Figure 2.** Comparison of the GABA<sub>A</sub> receptor responses as a function of recovery time reveals the persistence of the molecular memory. (A and B) The difference in current response to 500  $\mu\text{M}$  GABA for descending and ascending order dose applications, respectively. For  $t_{\text{exp}} = 100$  ms it takes less than 15 s, and for  $t_{\text{exp}} = 3$  s it takes at least 120 s before the difference in response is abolished. To determine the rate of decay of the memory and see if the memory function was sensitive to different application orders, the data was fitted to a single-exponential function. For descending doses the time constant was 8.2 and 79.4 s for  $t_{\text{exp}} = 100$  ms and 3 s, respectively. Ascending doses had time constants of 16.1 and 72.7 s for  $t_{\text{exp}} = 100$  ms and  $t_{\text{exp}} = 3$  s, respectively. For experiments with descending order of doses, the first response was used as the control response, but for the ascending doses a control response was recorded from the cell 180 s after the pulse train was applied (see inset under graph). Error bars are in SD.

majority of the receptor population into the fast desensitized state  $D_{\text{fast}}$ , which is more easily depopulated during  $t_{\text{wash}}$ , resulting in a slower accumulation of receptors residing in  $D_{\text{slow}}$  (Figure 3B). The number of free receptors available for subsequent exposures is thereby larger after exposure to high agonist concentrations. Simulated dose–response relationships for the open states (the arithmetic sum of  $O_1$  and  $O_2$ ) (Figure 3C) for  $t_{\text{exp}} = 100$  ms and 1 s, match the patterns from the experiments (Figure 1E). However, at longer  $t_{\text{exp}}$ , the model fails to reproduce the increasing difference between the ascending and descending application patterns. To remedy this we stabilized  $D_{\text{slow}}$  by reducing the exit rate from this state 6-fold. This slightly altered model accurately predicted the dose–response curves for both long and short  $t_{\text{exp}}$  (Figure 3D).

On the basis of the kinetic model and the CSPC experiments, an electronic equivalent circuit representing a population of GABA<sub>A</sub> receptors was constructed (Figure 3E). The receptor population is represented as charges on capacitors, and the

- (17) Sinclair, J.; Olofsson, J.; Pihl, J.; Orwar, O. *Anal. Chem.* **2003**, *75*, 6718–6722.
- (18) Jones, M. V.; Sahara, Y.; Dzuby, J. A.; Westbrook, G. L. *J. Neurosci.* **1998**, *18*, 8590–8604.
- (19) Lindquist, C. E.; Laver, D. R.; Bimir, B. *J. Neurochem.* **2005**, *94*, 491–501.
- (20) Onfelt, B.; Olofsson, J.; Lincoln, P.; Norden, B. *J. Phys. Chem. A* **2003**, *107*, 1000–1009.



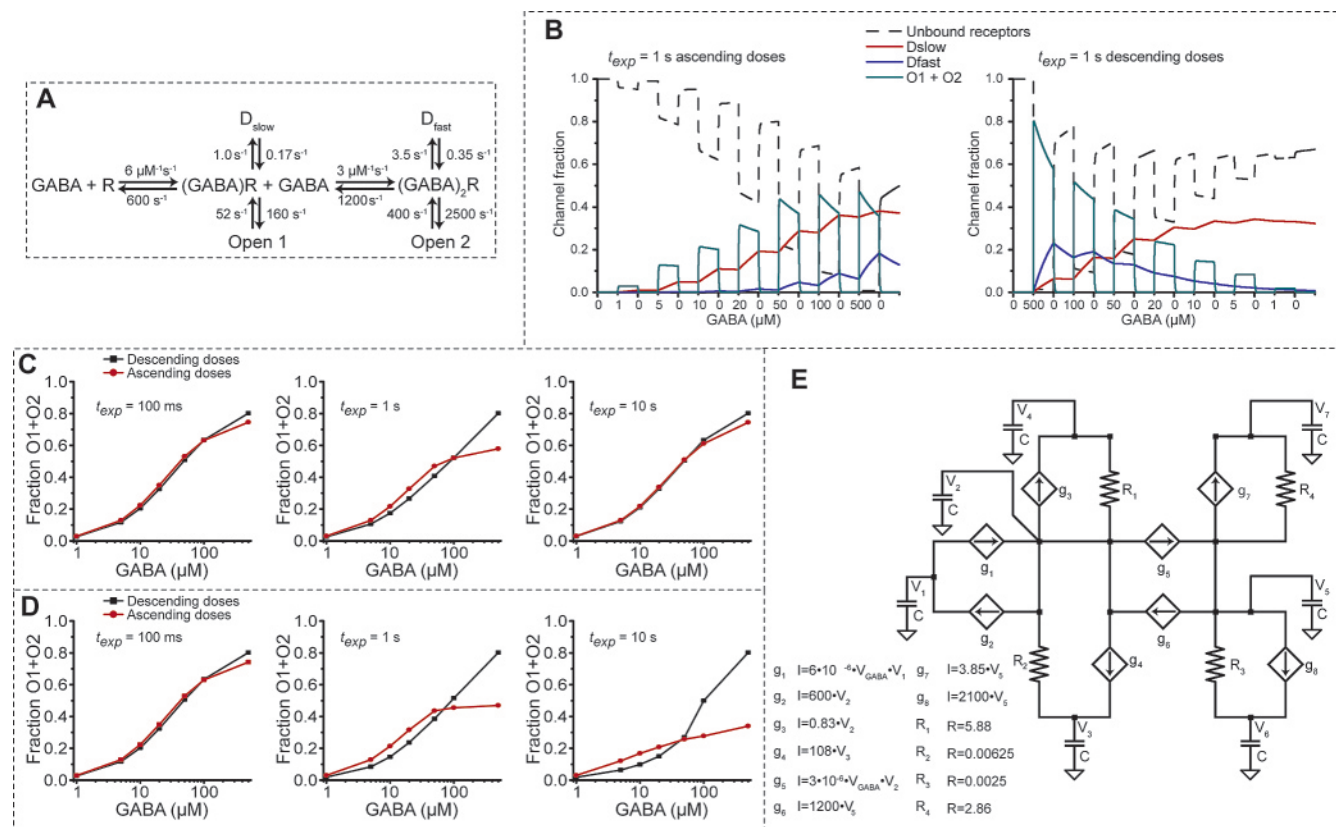


**Figure 3.** Modeling and simulation of the GABA<sub>A</sub> receptor molecular memory. (A) The kinetic model for the GABA<sub>A</sub> receptor, which the simulations were based on. (B) The simulated state distribution for  $t_{\text{exp}} = t_{\text{wash}} = 1 \text{ s}$  for applications in ascending and descending order of doses, respectively, reveals how the input function,  $f(t_{\text{exp}}, [\text{GABA}], t_{\text{wash}})$ , creates state distributions as a function of the microscopic rate constants. (C and D) Simulated dose–response curves for the open state ( $O_1 + O_2$ ) fractions using two different values for the exit rate from  $D_{\text{slow}}$ . In C the rate is from literature data, while in D the rate is calculated from our experimental data. The fraction of free receptors able to enter either  $O_1$  or  $O_2$  will be limited by  $D_{\text{slow}}$  for long exposures and by both  $D_{\text{slow}}$  and  $D_{\text{fast}}$  for short exposures and is also dependent on the order of application. (E) An equivalent circuit consisting of capacitors, resistors, and transconductors, representing a population of GABA receptors obeying the kinetic model in A. The concentration of GABA is represented as input voltages at two different points in the circuit, and the number of receptors in each of the states at a given time is represented as charges on the capacitors that can be read out as voltages  $V_1$ – $V_7$ , respectively.  $V_1$ , which represents the population of free receptors, is initially set to  $V_{\text{pop}}$ , representing the entire receptor population. The application of GABA will regulate the capacitor voltages in the circuit, and  $V_3$  and  $V_6$ , which represent the open states, can be considered as gate voltages applied to transistors where the membrane potential represents the supply voltage. This will result in an amplified signal equivalent to the current response obtained during the experiments.

distribution of the total charge among the capacitors describes the distribution among the states at each point in time. Since all capacitors have the same size, the capacitor voltages correspond to the number of receptors that currently reside in that state. Transitions between different states are controlled by resistors along with voltage-controlled current sources, transconductors, where the controlling voltage is the voltage for the state from which the charge is transferred. Finally, the applied GABA concentration can be considered as a voltage input,  $V_{\text{GABA}}$ , and it is thus possible to model the response from a population of receptors using SPICE simulations. The electronic equivalent circuit gives exactly the same result for state distributions as modeled using the kinetic scheme. The similarities in operating principle between a population of GABA<sub>A</sub> receptors under microfluidic control and a dynamic random access memory (DRAM) are striking. In a DRAM cell information is transiently stored in a capacitor and leaks out over time. In order for the memory to be maintained, readout and refreshment is periodically performed through an amplification circuit. The receptor-based memory presented here stores the history of exposure to activators in conformational states. The memory status changes over time and is accessed and

refreshed as the receptors are exposed to new doses of GABA provided by the microfluidic device.

It is well established that receptor desensitization is an important factor in regulating the receptor response in synaptic signaling,<sup>9,21–23</sup> and it has been proved that GABA<sub>A</sub> receptors can be temporarily arrested in different channel conformations and that the distribution of these states influences the way the receptor responds to subsequent stimuli.<sup>6,8,24,25</sup> We here show that a population of GABA<sub>A</sub> receptors themselves has the capability not only to receive information but also to store the information in conformational states. This is in stark contrast to previous views where receptors have been seen as receivers and transducers of information but not as data storage elements. One of the main concepts for neuronal computation calls for storage of memory in stationary states (point attractors),<sup>26</sup> and with our observations at hand, it is quite feasible that the

- Blitz, D. M.; Foster, K. A.; Regehr, W. G. *Nat. Rev. Neurosci.* **2004**, *5*, 630–640.
- Dajas-Bailador, F.; Wonnacott, S. *Trends Pharmacol. Sci.* **2004**, *25*, 317–324.
- Luscher, B.; Keller, C. A. *Pharmacol. Ther.* **2004**, *102*, 195–221.
- Overstreet, L. S.; Jones, M. V.; Westbrook, G. L. *J. Neurosci.* **2000**, *20*, 7914–7921.
- Bianchi, M. T.; Macdonald, R. L. *J. Neurosci.* **2001**, *21*, 9083–9091.
- Hopfield, J. J. *Proc. Natl. Acad. Sci. U.S.A.* **1982**, *79*, 2554–2558.

GABA<sub>A</sub> receptor (as well as other ligand-gated receptors) can function as such point attractors on time scales of milliseconds to minutes and function as distributors of synaptic weight within closely spaced areas of synapses. The experiments described here are performed with agonist exposure times longer than those found during synaptic transmission. However, it has been shown that repetitive applications of brief pulses of GABA (0.1–10 ms) also result in pronounced inhibition of GABA<sub>A</sub> receptors that accumulate in slowly desensitized states.<sup>8,11</sup> Furthermore, we describe how a microfluidic device can be used to control and program a biohybrid memory circuit. The device can exactly control the input function, and patch-clamp offers real-time readout of the processed current output.

Biohybrid memories may form the basis of large-scale integrated biocomputational devices and complex biosensors that not only respond to a stimulant but also have the capability to store this information. The interesting issue with such systems is not that they will compete with modern computers, but rather that they can work with chemical or physical input signals that can be of a great value for understanding and treating a medical

condition (e.g., a diagnostic tool, a drug screening platform or a model system) or alternatively identify threats to the human body (e.g., chemical and biological warfare agents). The feasibility of such systems is evident as large-scale integration of microfluidics<sup>27</sup> and computational microfluidics<sup>28</sup> have been demonstrated. Furthermore, parallel automated patch-clamp systems are now available,<sup>29</sup> and with appropriate microfluidic wiring these systems could be employed for such applications.

**Acknowledgment.** This work was funded by the Royal Swedish Academy of Science, the Swedish Research council (VR), The Göran Gustafsson Foundation, Cellectricon AB, and the Swedish Foundation for Strategic Research (SSF) through a donation from the Wallenberg Foundation

JA0580993

- 
- (27) Thorsen, T.; Maerkl, S. J.; Quake, S. R. *Science* **2002**, *298*, 580–584.  
(28) Chiu, D. T.; Pezzoli, E.; Wu, H. K.; Stroock, A. D.; Whitesides, G. M. *Proc. Natl. Acad. Sci. U.S.A.* **2001**, *98*, 2961–2966.  
(29) Zheng, W.; Spencer, R. H.; Kiss, L. *Assay Drug Dev. Technol.* **2004**, *2*, 543–552.